Mathematical Modelling and Analysis
Volume 12 Number 4, 2007, pages 441–458
 ISSN 1392-6292 print, ISSN 1648-3510 online

THERMAL PLASMA CUTTING. PART I: MODIFIED MATHEMATICAL MODEL

S. DASHKOVSKIY and A. NARIMANYAN

University of Bremen
Department of Mathematics and Computer Sciences, FB3
Center for Industrial Mathematics (ZeTeM)
P. O. 330440, D-28334 Bremen, Germany
E-mail: dsn@math.uni-bremen.de; arsen@math.uni-bremen.de

Received March 12, 2007; revised September 27, 2007; published online December 15, 2007

Abstract. The moving-boundary methodology with Stefan- and Signorini-type boundary conditions is used for the modelling of the thermal cutting of metals by a plasma beam. We model the problem as a coupled system of equations, the heat conduction equation with Signorini-type boundary conditions for calculating the temperature distribution in the workpiece, Stefan-type boundary condition for computing the unknown domain geometry and ODEs which account for the solid-solid phase transformations occurring due to the heat treatment of the material. For latter purpose a general model describing the kinetics of phase transformation is used. Finally, a model for computing the heat flux density absorbed by the cutting interface is derived using the data of emitted heat and radius of the plasma beam.

Key words: plasma cutting, solid phase transformation, moving boundaries, Stefan-Signorini boundary condition, interface kinetics, mathematical modelling

1. Introduction

Thermal cutting of metals is one of the production steps frequently used in heavy industry. It is of grate importance to achieve possibly high precision for the geometry of a cutout. This can minimize the subsequent machining costs. In this paper we deal with modelling of plasma cutting and present a model that takes phase transformations into account. This extends the modelling approach established in [22, 23].

The essential idea of cutting is to focus a lot of power onto a small area of surface of the material producing intense surface heating. First the material on the surface melts and then evaporates. As the vapour is puffed away or the molten metal is removed by the high speed gas flow, so a hole develops in the material. As the plasma cutting advances by melting, a characteristic feature

is the greater degree of melting towards the top of the workpiece resulting in top edge rounding and poor edge squareness. Top edge rounding is a slight rounding of the metal along the top edge of the cut and is mostly effected by material thickness. It is more apparent in thinner metals. The poor edge squareness causes additional difficulties on the next step in the manufacturing process (see Figure 1(b)). If the cut piece has to be welded, a high quality cut with square edges is especially important for the integrity of the weld.

Investigations are needed for the prediction and control of the above mentioned phenomena concerning the plasma arc cutting process. To get a quantitative description of the process, one requires a mathematical model for it. It must involve the different physical phenomena occurring in the workpiece during the cut, i.e. heat conduction, convection and radiation effects, mechanical deformations, phase transitions, etc. The model has then to be numerically simulated, and the results of the simulations have to be verified by experiments.

The modelling of this process is a complex mathematical problem. Several papers in the literature were devoted to this issue. In his pioneering work [25] on the mathematical theory of heat distribution during welding and cutting, Rosenthal outlines the fundamentals of the theory and derives analytical solutions for linear two- and three-dimensional flow of heat in solids. In their paper [13] Friedman and Jiang formulated the melting problem of a one-dimensional slab as a Stefan problem with Signorini boundary conditions at the moving boundary. Thereby they established existence and uniqueness theorems for the solution of the problem as well as studied the regularity and some geometric features of the free boundary. In [31] Bui An Ton considered the Stefan-Signorini problem with set-valued mappings in bounded domains where he imposed intersecting fixed and free boundary conditions. He proved the existence of a weak solution of Stefan-Signorini problem and showed the continuity of the moving interface. For further readings we refer to [14, 18, 19, 27, 28, 30]. Recently, a cutting model has been established by one of the authors of present manuscript [22], which encounters the temperature field analysis in the workpiece as well as the effects of cutting on the geometry of the cut pieces. In the work the author presents a numerical scheme for solving the cutting model using the adaptive finite elements method. The convergence of the implemented numerical algorithm is obtained as well (see [22]). In their later paper [23], the authors described models driven by two industrial applications, thermal cutting of metals and dynamics of aggressive reaction front in concrete-based materials, and illustrated the connection between these two models which is based on the presence of non-equilibrium conditions across the moving interface.

In the models derived in [22, 23] the effects of solid-solid phase changes were not taken into account. This is a very important issue, because due to the temperature changes a solid-solid phase transformation occurs in the material producing or absorbing some amount of heat energy. Therefore, in our present study we extend the cutting model of [22] by taking this phenomenon into account and using a kinetic model for the diffusional phase transformation in

form of ordinary differential equations. These equations are then coupled with the heat treatment problem.

The paper is organized as follows. Section 2 gives a brief description of the cutting phenomenon and outlines the problem under consideration. The phenomenon of phase transformation and some known models for its description are discussed in section 3. A new model for the kinetics of phase transformation taking the history of the temperature variation into account is developed in Section 4. Section 5 states an extended model for plasma cutting. A new model for the calculation of absorbed heat flux density by the cutting front is derived in section 6. We conclude with some remarks and outline for future work in section 7.

2. Problem Description and Physical Modelling

There is a wide range of thermal cutting techniques available for the shaping of materials. One example is the *plasma cutting*. The origin of the plasma-arc process goes back to 1941. In an effort to improve the joining of light metals for the production of aircraft, a new method of welding was born that used an electric arc to melt the material and a shield of inert gas around the electric arc to protect the molten metal from oxidation. Figure 1(a)[1] gives an impression on some typical applications of plasma cutting.

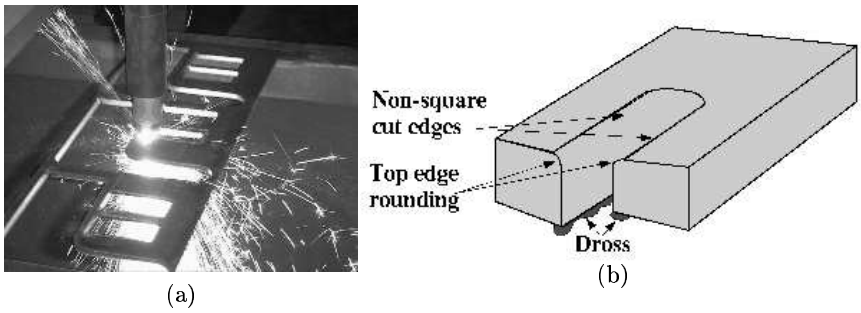

Figure 1. (a) An application of plasma cutting. (b) Some typical industrial problems.

Let consider a high-power plasma beam striking a small area of metal surface assumed to be homogeneous and isotropic. The material parameters such as density, heat capacity, conductivity, etc. of the workpiece are assumed to be constant. Figure 2 provides a schematic illustration of the plasma cutting process. The figure shows the plasma beam penetrating through the workpiece, the advancing hole and different physical phenomena taking place in the material.

[1] Pictures are taken from www.torchmate.com/automate/cncdemo.html and www.rtgstore.com/art

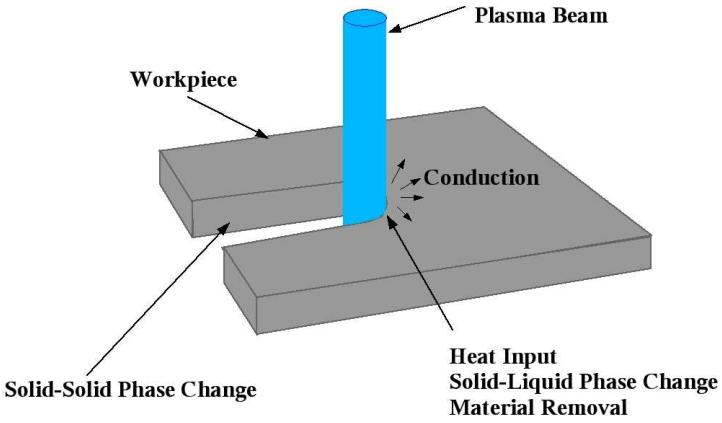

Figure 2. Schematic picture of thermal cutting.

The plasma beam is considered to be of cylindrical shape, and we assume that the heat flux from the plasma beam is emitted only in the normal direction to the surface of the cylinder. The heat lost by radiation is ignored. The plasma device moves at a constant velocity with respect to the workpiece and we assume that the heat flux density emitted by the plasma beam is constant and given. We do not consider the side effects caused by the smoke of the vaporizing metal. By side effects we mean that, for example, the evaporated material does not interfere with the incident plasma beam.

The first phenomenon we can observe is the absorption of the energy by the material. The absorption takes place within a thickness usually much less than a millimeter, so we can consider surface heating only. The temperature of the material surface does not rise infinitely. Part of the heat input from the plasma beam melts the metal resulting in solid-liquid phase change in the areas close to the source. When the material melts, latent heat is absorbed without any further rise in temperature. The second part of the heat is transferred into the workpiece by conduction from hotter to colder metal resulting in rise of the temperature in the material.

We consider a large piece of material, such that the heat exchange through the surface to the surrounding can be neglected in regard to the heat flow in the material itself. This assumption makes sense because the heat conductivity of metals is much greater than the heat transmission through the surface.

Another physical process is due to the fact that the plasma beam pierces through the workpiece with some constant velocity, while the high velocity gas flow removes the molten material from the bottom of the cut, or the kerf. As a result, the domain of interest changes in time resulting in a new unknown quantity.

Last, but not least, the so called solid-solid phase transformation takes place in the workpiece, which plays an important role in the modelling of the process. Due to the temperature changes, the material transforms from one solid phase to another producing or absorbing some amount of heat energy.

Before we formulate the problem in mathematical terms, let us write a few words about solid phase transitions and consider a modelling approach for this phenomenon.

3. Phase Transformation

Solid-solid phase transformations appear in different materials due to temperature changes. Typical example is the quenching of steel, where austenite transforms to pearlite, ferrite, cementite, bainite or martensite depending on alloy composition and cooling temperature range. This transformations lead to additional deformations due to density difference of these phases. Moreover the mechanical properties of these materials are different. The rate of cooling determines the relative proportions of these phases and therefore the mechanical properties of a workpiece.

The formation of austenite during heating of a workpiece consumes heat energy. The transformation of austenite to other phases emits heat energy. Hence, this phenomenon should be taken into account for the determination of the temperature in the workpiece.

In this paper we assume that only diffusional phase transformation takes place. This is not restrictive if we consider a steel workpiece with a low martensitic fraction in the initial state. In this case first the austenitic phase will form in some regions due to heating by plasma. Then the cooling of material after cutting is relatively slow and we may assume that the austenite transforms to only one phase, say pearlite.

It is commonly accepted that the diffusion phase transformation processes are controlled by nucleation and growth of nuclei, where impingements should be taken into account. First equations based on the analysis of these two effects were obtained in the pioneering papers for the isothermal case. The result of Johnson and Mehl [16], derived originally for the pearlite formation from austenite, reads as follows

$$p(t) = 1 - e^{-\frac{\pi}{3} N_\nu G^3 t^4}, \tag{3.1}$$

where $p(t)$ is the volume fraction transformed up to the moment t. N_ν is the rate of nucleation and G is the rate of the radial growth, both supposed to be constant throughout the reaction.

Criticizing the assumption of the rate of nucleation constance Avrami [3] starts with the assertion that the new phase is nucleated by tiny germ nuclei which exist already in the parent phase, whose effective number $\bar{N}$ depends on the temperature and duration of the superheating, generally decreasing with increase of either. Denoting by G the averaged rate of growth of the linear dimension of a nucleus, Avrami gets the following kinetic equation for the polyhedral growth

$$p(t) = 1 - e^{-\sigma G^3 \bar{N} t^3}, \tag{3.2}$$

where σ is a shape factor (equal to $\frac{4\pi}{3}$ for a sphere, e.g.). We would like to emphasize that in these equations the parameters G and N_ν (or $\bar{N}$) reflect

two different effects, namely growth and nucleation respectively. However in the isothermal case one can write

$$p(t) = 1 - e^{-Kt^4}$$

with $K = \frac{\pi}{3} N_\nu$ instead of (3.1) or

$$p(t) = 1 - e^{-Kt^3}, \tag{3.3}$$

with $K = \sigma G^3 \bar{N}$ instead of (3.2). Later, paved by Avrami, who stated that the power of t in (3.3) varies from 3 to 4 (for the polyhedral growth), it led to the generalized Johnson-Mehl-Avrami (JMA) equation

$$p(t) = \overline{p}(1 - e^{-Kt^n}) \tag{3.4}$$

which proved itself to be in a good agreement with most of isothermal experiments. Here $\overline{p}$ is the equilibrium fraction reached at constant temperature θ after an infinitely long time. The parameters K and n depend on temperature and can be determined from the isothermal time-temperature transformation diagram. We also refer to [6] and [7] for further details and explanations.

In practice it is impossible to reach the prescribed temperature instantaneously. If transformation starts already in the beginning of quenching and goes fast, the equation (3.4) can not be used at least for the early stage of reaction. To describe the incubation period at the start of transformation the additivity rule was proposed by Scheil [26]. Later it was used for the entire transformation in the non-isothermal case, see e.g. [15]. Let $\tau(p, \theta)$ be the time needed to reach the p fraction in the isothermal transformation process at temperature θ, then by the additive rule in a non-isothermal process $\theta(t)$ the fraction p is reached at the moment t such that

$$\int_0^t \frac{ds}{\tau(p, \theta)} = 1.$$

For the experimental investigation of this rule we refer to the paper of Wever and Krisement [32], for some theoretical investigation of its applicability see, e.g., [12]. Some generalizations can be proposed. As it is known from experiments that the rate of transformation varies essentially in course of reaction even at constant temperature being much higher at the middle stage as at the beginning or at the end. Hence different τ-s should be weighted for different stages:

$$\int_0^t \frac{ds}{\tau(p, \theta) f(s, \theta)} = 1,$$

where f is a nonnegative weighting function. See also [24] for other modifications.

In order to treat non-isothermal transformations the differential form of the JMA equation

$$\frac{dp}{dt} = \overline{p} n K t^{n-1} e^{-Kt^n} \tag{3.5}$$

obtained from (3.4) taking time derivative is often used, or sometimes written in an autonomous form:

$$\frac{dp}{dt} = nK^{\frac{1}{n}} \Big(-\ln\Big(1 - \frac{p}{\overline{p}}\Big)\Big)^{1-\frac{1}{n}} (\overline{p} - p), \tag{3.6}$$

where the factor $(\overline{p} - p)$ may be regarded as a retardation factor due to impingements. Austin and Ricketts [2] have got a better agreement with experiment with retardation factor $(\overline{p}-p)^2$. Trying to get some higher accuracy, numerous generalizations of this equation, also combined with Scheil's rule, have been proposed. We refer to the papers [4, 11, 24] where different equations and iteration procedures of such type are discussed and compared on the base of experiments (in the last two papers) performed on the 100Cr6 steel. It seems that one can always find an appropriate modification of (3.5) or (3.6) for a given steel which is in a good agreement with experiment for a certain class of temperature variations, but another equation should be taken if temperature changes in a different way, say, if the temperature rate is essentially different. We believe that this imperfectness is caused by the fact that the coefficient K appearing in (3.4) can not reflect both temperature dependent processes of nucleation and growth, whereas variation of n brings not so much improvement of the model. Indeed, in (3.1) and (3.2) the corresponding parameters appear as a product in K, hence instead of these two (of nucleation and growth) we have only one parameter K.

The manufacturing processes in industry as for example plasma cutting of metal are often non-isothermal and the temperature rate may vary drastically. Some essentially new models for the phase evolution are needed which could embrace a wide range of temperature variations. This is the motivation of the investigations presented here. We believe that some parameters controlling the nucleation and growth should be used explicitly. It is also recognized that the history of temperature variation should be taken into account (see [11, 17, 20], e.g.), since the transformed fraction does not depend on time and temperature as their function. For example in [20, 21] a path dependent parameter β is introduced and the product fraction is assumed to be a function of β. In the following we introduce a new approach for the phase transformation kinetics modelling.

4. Kinetics of Phase Transformation

Let the temperature $\theta(t)$ be a given function of time. Let us consider V_{t_0} the (micro-)volume of the nucleus of the product phase that has been appeared at the time instant t_0 in a macrovolume V. We introduce a microparameter $\pi = V_{t_0}/V$, which is the contribution to the volume fraction p of the new transformed phase. After the overcoming of the energetic barrier this volume V_{t_0} will grow depending on time t and current temperature $\theta(t)$. In order to

take into account the history of this process we assume that the value of π is a functional of the temperature:

$$\pi(t_0, t) = F_\theta(t_0, t).$$

The sum over all such microvolumes appeared up to the current moment t yields the volume fraction

$$p(t) = \sum_{t_0} \pi(t_0, t) \tag{4.1}$$

of the product phase in the macrovolume V. We denote by N the number of nuclei in the volume V. We assume that the nucleation rate $\dot{N}$ depends on time, temperature and current value of the fraction of the new phase

$$\dot{N} = \eta(t, \theta(t), p).$$

Writing the sum in (4.1) as an integral over the moments of birth of each nucleus we have the following expression for the volume fraction

$$p = \int_0^t F_\theta(t_0, t)\eta(t_0, \theta(t_0), p)\, dt_0, \tag{4.2}$$

where the integration is taken over the "birth" times t_0 of new nuclei. We assume further that the growth of the microparameter π can be described by the following differential equation

$$\frac{d\pi}{dt} = G(t_0, t, \pi, p, \theta) \tag{4.3}$$

with the initial condition

$$\pi(t_0) = \pi^0, \tag{4.4}$$

where G is some given function and π^0 is the critical value of the microparameter π characterized by the critical radius of the appeared volume needed to overcome the energy barrier. Let us differentiate (4.2) over the time

$$\frac{dp}{dt} = \pi^0\eta(t, \theta, p) + \int_0^t G(t_0, t, \pi, p, \theta)\eta(t_0, \theta, p)\, dt_0, \tag{4.5}$$

where we have used (4.3) and (4.4). The first term of the right side is the contribution to the fraction rate of new critical volumes appearing at the moment t with the rate $\eta(t, \theta(t), p(t))$, whereas the second corresponds to the growing process of already existing ones.

Assuming that G is linear with respect to π

$$G(t_0, t, \pi, p, \theta) = A(t, p, \theta)\pi(t_0, t) + B(t, p, \theta)$$

and substituting it into equation (4.5) we obtain the following system of differential equations describing the phase evolution

$$\begin{cases} \dfrac{dp}{dt} = \pi^0 \eta(t,\theta,p) + A(t,p,\theta)p + B(t,p,\theta)N, \\ \dfrac{dN}{dt} = \eta(t,\theta,p). \end{cases} \tag{4.6}$$

We emphasize that π^0, p, N and η have a clear physical meaning. Some concrete expressions for π^0 and η can be deduced from some deeper physical considerations or experiments. For example for the austenitisation in [17] the nucleation rate was taken as Arrhenius term

$$\eta = N_0\, e^{-Q_N/R\theta},$$

with N_0 as temperature independent rate, Q_N as the temperature independent activation energy for nucleation and R as the gas constant. As for functions A and B, some examples for these coefficients with corresponding explanations are given in [8].

System (4.6) can be simplified in some particular cases applying some further assumptions, see [8] for several examples leading to known models, such as of Leblond, Johnson-Mehl-Avrami or isokinetic equation.

The phase transformation model (4.6) describes the kinetics of a phase change in a point. It can be used for any kind of diffusional phase transformation. With help of this model the mathematical statement of the problem is given in the next section.

5. Modified Cutting Model

Let Ω be an open and bounded domain in $\mathbb{R}^n$, $n = 2, 3$, initially occupied by the workpiece. The boundary $\partial\Omega$ of the domain is assumed to be of class $\mathbb{C}^{0,1}$. Let $0 < T < +\infty$ be given, denote by $\theta(x,t)$ the temperature of the workpiece and I the time interval $(0,T)$. The initial temperature distribution of the workpiece is given by $\theta_0(x)$, which is less than the melting temperature at all points. For every $t \in I$ the domain Ω is assumed to consist of two non-intersecting parts, namely $\overline{\Omega} = \overline{\Omega_s(t)} \cup \overline{\Omega_c(t)}$, where $\Omega_s(t)$ and $\Omega_c(t)$ are the domains occupied by the solid part of the workpiece and cut cavity at a time instant t, respectively.

At any point x in $\Omega_s(t)$ the heating by plasma beam leads to the temperature growth as long as the plasma beam comes closer to that point until the temperature reaches its maximum value at a certain time instant. After this the temperature at the point x decreases as the beam moves away from it. Hence, we may assume that the temperature profile at any point $x \in \Omega_s(t)$ has the form of a graph illustrated in Figure 3. For simplicity, we assume that there may exist only two solid phases in the workpiece, say austenite and pearlite. Let θ_a be the critical temperature such that over that value the transformation from the first phase (pearlite) to the second one (austenite) starts. Below the temperature θ_a the second phase (ausentite) is unstable and immediately transforms to perlite as the workpiece cools down. If the line $\theta = \theta_a$ crosses the temperature profile $\theta(x,t)$ at two points, denoted by

$\tau_1(x)$ and $\tau_2(x)$ respectively, see Figure 3, then the transformation of pearlite to austenite starts at the moment $\tau_1(x)$ and lasts till $\tau_2(x)$. After the time instant $\tau_2(x)$, the austenite starts to transform back to pearlite. If the line $\theta = \theta_a$ do not crosses the temperature profile or only touches it at one point, then there will be no phase transformations at x.

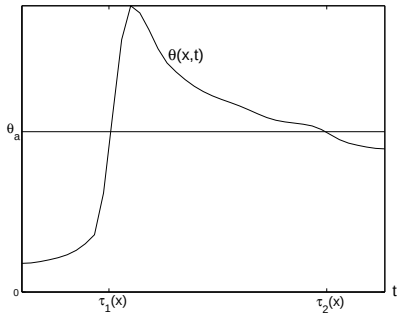

Figure 3. Typical temperature profile at a point x.

Now, equations (4.6) can be used to model the described solid-solid phase changes. They are derived for a point, the space coordinates of which can be taken as parameters in model equations (4.6). Let $p(x,t)$ and $a(x,t)$ denote the volume fractions of pearlite and austenite at a point x and time t. Certainly, the condition $p(x,t) + a(x,t) = 1$ holds.

Consider an arbitrary point $x \in \Omega_s(t)$. Obviously, no phase changes will take place for $t \in (0, \tau_1(x))$. After $t = \tau_1(x)$ the transformation to austenite is described by

$$\begin{cases} \dfrac{da}{dt}(x,t) = \pi_1^0 \eta_1(t, \theta(x,t), a) + A_1(t, a, \theta(x,t))a + B_1(t, a, \theta(x,t))N_a, \\ \dfrac{dN_a}{dt}(x,t) = \eta_1(t, \theta(x,t), a), \end{cases}$$

with initial conditions $a(x, \tau_1(x)) = 0$ and $N_a(x, \tau_1(x)) = 0$, where A_1 and B_1 are given material functions. These equations should be solved on the time interval $(\tau_1(x), \tau_2(x))$. The obtained solution of the system provides us with the initial condition for the backwards transformation to pearlite, which itself may be described via similar model equations, which are valid in the time interval $(\tau_2(x), T)$:

$$\begin{cases} \dfrac{dp}{dt}(x,t) = \pi_2^0 \eta_2(t, \theta(x,t), p) + A_2(t, p, \theta(x,t))p + B_2(t, p, \theta(x,t))N_b, \\ \dfrac{dN_b}{dt}(x,t) = \eta_2(t, \theta(x,t), p), \end{cases}$$

where A_2 and B_2 are given material functions. Accordingly, the initial conditions are $p(x, \tau_2(x)) = 1 - a(x, \tau_2(x))$ and $N_b(x, \tau_2(x)) = 0$. These equations

should be coupled with the heat equation, since functions entering the right-hand sides are depending on the temperature distribution in the workpiece and, visa versa, the temperature is influenced by heat energy emission or consumption during phase transformations.

Now, let $\partial\Omega_s(t)$ be the boundary of the time dependent domain $\Omega_s(t)$ at time t (free interface) and we assume that $\partial\Omega_s(t)$ is a Lipschitz curve. By ν we denote the unit outward normal vector of the domain $\Omega_s(t)$. Let j_{abs} be the heat flux density (heat flux per unit surface) absorbed by the melting interface due to the heat radiated by the plasma beam. In addition to the terms defined above we use the following notation: ρ is the density of the workpiece, c_s is the specific heat, k is the heat conductivity of the material, L_m is the latent heat of melting, L_a, L_p are the latent heats of the solid-solid phase transformation to austenite and to pearlite, respectively; θ_m is the melting temperature, $v \geq 0$ is the velocity of the melting front.

Assuming that no heat exchange can happen between the workpiece and the exterior through $\partial\Omega_s(t)$, the modified mathematical model, governing the cutting process with solid-solid phase changes, is the following:

Problem 1. [Modified Cutting Model] Find the function $\theta(x,t) \in \mathbb{C}_1^2(\Omega_s \times I) \cap \mathbb{C}(\overline{\Omega_s \times I})$, representing the temperature of the body, the piecewise smooth surface $\partial\Omega_s(t)$ representing the free boundary of the solid domain $\Omega_s(t) = \{x;\ \theta(x,t) < \theta_m\}$ and continuous functions $a(x,t)$ and $p(x,t)$, representing the volume fractions of austenite and perlite, such that

$$\rho c_s \frac{\partial\theta}{\partial t} = \nabla \cdot (k\nabla\theta) - \rho L_a \frac{da}{dt} + \rho L_p \frac{dp}{dt} \qquad x \in \Omega_s(t), \quad t \in I, \tag{5.1}$$

$$\frac{da}{dt}(x,t) = \pi_1^0 \eta_1(t,\theta(x,t),a) + A_1(t,a,\theta(x,t))a + B_1(t,a,\theta(x,t))N_a \tag{5.2}$$
$$\text{for } x \in \Omega_s(t), \quad t \in (\tau_1(x),\tau_2(x)),$$

$$\frac{dN_a}{dt}(x,t) = \eta_1(t,\theta(x,t),a), \qquad x \in \Omega_s(t), \quad t \in (\tau_1(x),\tau_2(x)), \tag{5.3}$$

$$\frac{dp}{dt}(x,t) = \pi_2^0 \eta_2(t,\theta(x,t),p) + A_2(t,p,\theta(x,t))p + B_2(t,p,\theta(x,t))N_b \tag{5.4}$$
$$\text{for } x \in \Omega_s(t), \quad t \in (\tau_2(x),T),$$

$$\frac{dN_b}{dt}(x,t) = \eta_2(t,\theta(x,t),p), \qquad x \in \Omega_s(t), \quad t \in (\tau_2(x),T), \tag{5.5}$$

with the following boundary conditions on $\partial\Omega_s(t)$:

$$\theta \leq \theta_m, \quad j_{abs} - k\nabla\theta \cdot \nu \geq 0, \tag{5.6}$$
$$(\theta - \theta_m)(j_{abs} - k\nabla\theta \cdot \nu) = 0,$$

called the *Signorini-type* boundary conditions and

$$k\nabla\theta \cdot \nu - \rho L_m v \cdot \nu = j_{abs}, \tag{5.7}$$

named the *Stefan-type* boundary condition.

As for the initial conditions, we set

$$\begin{aligned} &\theta(x,0) = \theta_0(x) < \theta_m \qquad x \in \Omega, \\ &\Omega_s(0) = \Omega, \\ &a(x,\tau_1(x)) = 0, \quad p(x,\tau_2(x)) = 1 - a(x,\tau_2(x)), \\ &N_a(x,\tau_1(x)) = 0, \quad N_b(x,\tau_2(x)) = 0. \end{aligned} \tag{5.8}$$

Remark 1. The terms $\rho L_a \dfrac{da}{dt}$ and $\rho L_p \dfrac{dp}{dt}$ in (5.1) represent the heat consumption by the phase transformation from pearlite to austenite (consumption, hence with minus sign in (5.1)) and emission due to the inverse transformation from austenite to pearlite, respectively.

Note, that Signorini boundary conditions (5.6) are non linear. At each fixed instant t there exist two regions: in one region we have heating phase, on the other melting phase. Moreover, these regions are not prescribed, resulting in a moving boundary problem. The molten material is immediately removed by an assisting gas, thus, the heat flux applies to the free boundary directly. When the temperature on the cutting front becomes less than the melting temperature, the front stops moving. As a result, on the moving boundary, either the temperature is less than the melting temperature or it is equal to the melting temperature and the cutting front moves with a positive velocity. So, for the cutting model we have alternative types of boundary conditions on the unknown moving interface $\partial\Omega_s(t)$:

$$\theta < \theta_m, \quad j_{abs} - k\nabla\theta \cdot \nu = 0, \quad v = 0$$

or

$$\theta = \theta_m, \quad j_{abs} - k\nabla\theta \cdot \nu > 0, \quad v > 0.$$

For more detailed explanation of the cutting model and Stefan-Signorini boundary conditions we refer to [23]. We call the problem (5.1)–(5.8) *the modified thermal-cutting model* and note that the developed mathematical model is rather general and does not depend on the type of cutting. The main difference between different cuttings is the amount of energy absorbed by the workpiece, which depends on the thermo-physical properties of the material as well as on the several parameters of the heat source.

In this model we are mainly concerned with the problem of heat transfer and temperature distribution in the workpiece during the thermal plasma cutting. The problem is solved, if at any moment the temperature of every point of the workpiece and the geometry of the workpiece are identified.

The heat flux density j_{abs} and v are equal to zero on the part of boundary where no heat input takes place. Therefore, on that part of the boundary we have homogeneous Neumann conditions. The idea behind the Stefan-type boundary condition is relatively simple; the total heat flux absorbed by the interface is divided into two parts: one part is conducted and the other part is used to melt the material. A model for calculating the heat flux density j_{abs} absorbed by the cutting front is derived in the following section.

6. Modelling of Absorbed Heat Flux Density

A feature common to most plasma and laser cutting processes is that they occur as a result of removing the material by melting and/or vaporizing as intense laser light or a high-temperature, partially ionized plasma gas stream interacts with the material surface. The amount of heat generated by plasma arc or laser beam plays a very important role in the kinetics of thermal cutting processes. Let us first present some earlier studies on the matter.

In relation to the measurable quantities (current voltage and power) Rosenthal [25] has made a study of the plasma arc and found that the energy delivered to the workpiece Q_w represents about 65% of the total energy Q_t supplied by the arc. We express it in formula by

$$Q_w = 0.65 Q_t = 0.65 \cdot const \cdot V\, I_c,$$

where V is the voltage drop in arc and I_c is the current intensity. Rosenthal discussed three types of moving heat sources: point source, line source and plane source. For each type of heat source he gave the relation between the temperature distribution and the heat Q_w delivered to the workpiece. For example, in the case of a point source the relation obtained is the following

$$\theta - \theta_0 = \frac{Q_w}{2\pi k} e^{-\lambda v \xi}\, \frac{e^{-\lambda v r}}{r},$$

where $\xi = x - vt$, $1/2\lambda = k/\rho c_s$ and r is the radius of the plasma beam. Note, that this relation is valid only below $\theta = \theta_m$.

Arai et al. [1] described two categories of heat flux density measurements: i) indirect, measurements made by calculating heat transfer rates, using fundamental theories together with measurements of temperature and thermo physical properties, and ii) direct measurements using heat flux density sensors placed in the thermal field.

In the model of Schulz et al. [27] the heat flux density absorbed at the boundary is proportional to the laser beam intensity $\mathcal{I}$ via the absorption coefficient A_p:

$$j_{abs} = -A_p \mathcal{I} e_z \cdot \nu,$$

where $e_z \cdot \nu$ is the angle of incidence of the laser beam and j_{abs} is, as usual, the heat flux density absorbed by the workpiece. The laser beam intensity $\mathcal{I}$ itself is characterized by the maximum intensity of the beam $\mathcal{I}_0$ and the beam radius r:

$$\mathcal{I} = -\mathcal{I}_0(t) f\Big(\frac{x - v_0 t}{r}\Big),$$

where v_0 is the speed of feeding (the speed of the moving laser) and f is a given distribution ($0 \le f \le 1$).

Bunting et al. [5] developed a relationship between the power density incident on a material and the cut speed in terms of the thermal properties of the material. They used the technique of Rosenthal on moving heat sources and got the relation

$$\frac{j_e}{h} = \frac{2k(\theta_m - \theta_0)}{r^2} \frac{1}{\mathcal{I}(s)},$$

where j_e is the heat flux density emitted from the surface of the heat source, h is the thickness of the material and $s = \dfrac{vr}{2\alpha}$ with α being the heat diffusivity. The value of $\mathcal{I}(s)$ has been calculated by authors and could be expressed via

$$\mathcal{I}(s) = \int_0^1 r' dr' \int_0^{2\pi} \exp(-sr' \cos\phi) K_0 s \left(r'^2 - 2r' \sin\phi + 1 \right)^{1/2} d\phi,$$

where K_0 is the zeroth order modified Bessel function of the second kind and the equation is written in cylindrical coordinates (r', ϕ) with dimensionless r'.

In studying the heat-affected zone during the laser cutting of stainless steel, Sheng et al. [29] expressed the beam energy $E_b(x, y)$ as a function of spatial coordinates via the beam intensity $\mathcal{I}(x, y)$ of Gaussian type

$$E_b(x, y) = \int \mathcal{I}(u, y) \frac{du}{v} = \int \frac{A(u, y)P}{\pi r^2 v} \exp\Big(- \frac{u^2 + y^2}{r^2} \Big) du,$$

where A is the absorptivity and P is the beam power.

In the following we describe a simple technique to calculate the heat flux density on the absorbing surface. For calculations it is convenient to discuss

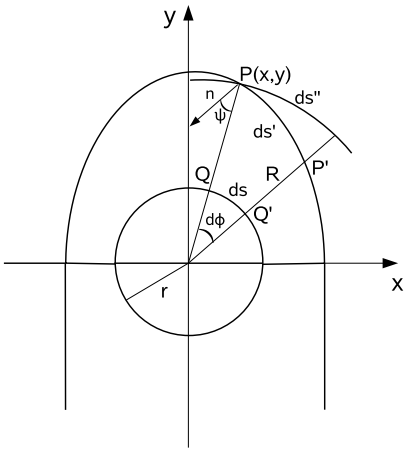

Figure 4. Emitted and absorbed heat flux density.

the topic not in terms of point source, but in terms of incremental surface elements. Therefore consider, as illustrated in Figure 4, a small emitting surface of area (length) ds, where the point Q is located. Further, let us assume that the cylindrical surface of the plasma beam is emitting heat in the radial

direction, i.e. the heat flux density vector at any point of the beam surface has the direction of the normal to the plasma surface at that point.[2]

We denote by j_e the heat flux density (the quantity of heat flowing across a unit area) emitted from the arbitrary point Q of the surface of the plasma jet, by j_{abs} the heat flux density absorbed at the point P of the surface of the workpiece due to the emission from Q and by r the radius of the plasma beam. Assuming that the heat flux density j_e at the point Q and the radius r of the beam are given, our aim is to calculate the heat flux density absorbed at the point P of the workpiece surface (see Figure 4).

Let dq be the rate at which the energy leaves the incremental area ds. Then the average flux j_e^{av} leaving ds is defined as

$$j_e^{av} = \frac{dq}{ds}, \tag{6.1}$$

and the flux due to the point Q on the beam surface is defined to be

$$j_e = \lim_{ds \to 0} \frac{dq}{ds}. \tag{6.2}$$

The flux emitted from ds is then completely absorbed (assume the material is a black body) by the surface of the material, more precisely, by the part of the surface which we denote by ds'. Then analogously to (6.1), the average heat flux density j_{abs}^{av} absorbed by ds' is

$$j_{abs}^{av} = \frac{dq}{ds'}$$

and owing to (6.2) we obtain

$$j_{abs} = \lim_{ds' \to 0} \frac{dq}{ds'} = \lim_{ds' \to 0} \frac{j_e ds}{ds'}. \tag{6.3}$$

For cylindrical heat source we have

$$ds = r d\phi,$$

where $d\phi$ is the incremental angle between the lines connecting points P and P' with the center of the beam (see Figure 4).

Now let ds'' be an element of the spherical surface which we obtain by projecting ds' normal to the direction PQ (the direction that the point P makes with the emitting point Q). In terms of the drawings in Figure 4, the flux at the point P due to the energy leaving the point Q may be determined in terms of energy falling on the element ds'' of the circular surface (center at origin, radius R) which passes through P. We then obtain for the surface element ds''

$$ds'' = ds' \cos\psi \quad \text{as} \quad d\phi \to 0,$$

[2] This assumption is made only for simplicity, the calculations can be also done for other flux density distributions.

where ψ is the angle between the normal of the workpiece surface at point P and the line PQ. Thus, we acquire

$$ds' = \frac{ds''}{\cos\psi}. \tag{6.4}$$

If, for example, the interface is represented via a smooth graph, $y = f(x)$, then we can express $\cos\psi$ as

$$\cos\psi = -\frac{1}{\sqrt{x^2+f^2(x)}}\begin{pmatrix} x \\ f(x)\end{pmatrix}\cdot\frac{1}{\sqrt{1+(f'(x))^2}}\begin{pmatrix} f'(x) \\ -1\end{pmatrix}, \tag{6.5}$$

where $\frac{1}{\sqrt{x^2+f^2(x)}}\begin{pmatrix} x \\ f(x)\end{pmatrix}$ represents the unit normal vector to the surface ds'' at point $P(x,y)$ and $\frac{1}{\sqrt{1+(f'(x))^2}}\begin{pmatrix} f'(x) \\ -1\end{pmatrix}$ denotes the unit normal to the graph $y = f(x)$ at point $P(x,y)$.

Inserting the expressions for ds' from (6.4) and $\cos\psi$ from (6.5) with $ds'' = Rd\phi$ into (6.3), and taking into account that $ds' \to 0$ is in fact equivalent to $d\phi \to 0$, we obtain

$$\begin{aligned} j_{abs} &= -j_e \cdot \lim_{d\phi\to 0} \frac{rd\phi\left(\sqrt{x^2+f^2(x)}\right)^{-1}\left(\sqrt{1+(f'(x))^2}\right)^{-1}(xf'(x)-f(x))}{Rd\phi} \\ &= -j_e r\frac{xf'(x)-f(x)}{(x^2+f^2(x))\sqrt{1+(f'(x))^2}}. \end{aligned}$$

In general, the expression for $\cos\psi$ can be written in the form

$$\cos\psi = n\cdot\nu_r,$$

where ν_r is the unit vector at the point P pointing in the direction of the emitting point Q. Therefore, for general absorbing surfaces the heat flux on the moving front takes the form

$$j_{abs} = j_e\frac{r}{d_p}\cdot n\cdot\nu_r, \tag{6.6}$$

where d_p is the distance between the point P and the center of plasma beam. The derived expression (6.6) provides a method to compute the pointwise heat flux density and can be effectively used in the numerical treatment of the modified cutting model.

7. Discussion and Conclusions

We have presented a model describing the heat process in workpiece due to plasma cutting. The temperature distribution and the geometry of the

workpiece can be determined with this model. The latent heat of the solid-solid phase transformation has been taken into account, which extends the model developed in [22]. Numerical implementation of the modified model and simulation results will be published in the second part of this work.

We would like to mention that the temperature field analysis and computation of the geometry of the cut pieces is the first step on the way of the modelling of the whole plasma cutting process. Further steps include the determination of thermoelastic, thermoplastic deformations as well as the deformations due to phase transformations. A general modelling framework for the case of finite deformations taking phase transformations into account was presented in [9, 10]. The cutting model established in this paper should be further coupled with a thermoplastic model and transformation induced plasticity.

References

[1] N. Arai, A. Matsunami and S. W. Churchill. A review of measurements of heat flux density applicable to the field of combustion. *Experimental, Thermal and Fluid Science*, **12**, 452–460, 1996.

[2] J.B. Austin and R.L. Ricketts. Kinetics of the decomposition of austenite at constant temperature. *Trans. A.I.M.E.*, **135**, 396–415, 1939.

[3] M. Avrami. Kinetics of phase change. II. *J. of chemical physics*, **8**, 212–224, 1940.

[4] M. Böhm, M. Hunkel, A. Schmidt and M. Wollf. Evaluation of various phase-transition models for 100cr6 for application in commercial FEM programs. *J. de Physique IV*, **120**, 581–589, 2004.

[5] K. A. Bunting and G. Cornfield. Toward a general theory of cutting: A relationship between the incident power density and the cut speed. *Transactions of the ASME*, **116**, 1975.

[6] J. Burke. *The kinetics of phase transformation in metals.* Pergamon press, 1965.

[7] J. W. Christian. *The theory of transformations in metals and alloys.* Pergamon press, 1965.

[8] S. Dachkovski. Evolution of diffusional phase transformation with varying temperature. In: *Proc. Of 3rd International Conference Computational modeling and simulation of materials*, Sicily, Italy, 265–272, 2004.

[9] S. Dachkovski and M. Böhm. Finite thermoplastisity with phase changes based on isomorphisms. *Int. J. Plast.*, **20**, 323–334, 2004.

[10] S. Dachkovski and M. Böhm. Modeling of elastoplastic materials with phase changes. *J. de Physique IV*, **120**, 153–160, 2004.

[11] S. Dachkovski, M. Böhm, A. Schmidt and M. Wolff. Comparison of several kinetic equations for pearlite transformation in100cr6 steel. Berichte aus der technomathematik, ZeTeM, University of Bremen, 2003.

[12] A. Fasano and M. Primicerio. An analysis of phase transition models. *Europ. J. Appl. Math.*, **7**, 439–451, 1996.

[13] A. Friedman and L. Jiang. A Stefan-Signorini problem. *J. Differential Equations*, **51**, 213–231, 1984.

[14] H. Hafercamp, M. Niemeyer, J. Hoerner, J. Bosse, M. Kock and F. Könemann. Numerical modelling of thermal plasma cutting. In: *Thermal cutting conference*, Timisoara, 1999.

[15] D. Hömberg. A mathematical model for the phase transitions in eutectoid carbon steel. *J. of Appl. Math.*, **54**, 31–57, 1995.

[16] W. Johnson and R. Mehl. Reaction kinetics in processes of nucleation and growth. *Trans. AIME*, **315**, 416–441, 1939.

[17] A. T. W. Kempen, F. Sommer and J. E. Mittemeijer. Determinetion and iterpretation of isothermal and non-isothermal kinetics; the effective activation energies in terms of nucleation and growth. *J. Mat. Sci.*, **37**, 1321–1332, 2002.

[18] M. Kim. Transient evaporative laser-cutting with boundary element method. *Journal of Applied Mathematical Modelling*, **25**, 25–39, 2000.

[19] K. Matsuyama. Mathematical modelling of kerf formation phenomena in thermal cutting. *Welding in the World*, **39**(1), 28–34, 1997.

[20] J. E. Mittemeijer. Review analysis of the kinetics of phase transformations. *J. Mat. Sci.*, **27**, 3977–3987, 1992.

[21] J. E. Mittemeijer and F. Sommer. Solid state phase transformation kinetics: a modular transformation model. *Z. Metallkd.*, **93**, 352–361, 2002.

[22] A. Narimanyan. *Stefan-Signorini moving boundary problem arisen from thermal plasma cutting: mathematical modelling, analysis and numerical solution.* PhD thesis, ZeTeM, Faculty of Mathematics, University of Bremen, 2006.

[23] A. Narimanyan and A. Muntean. Mathematical modelling driven by two industrial applications: A moving boundary approach. *Mathematical Modelling and Analysis*, **11**, 295–314, 2006.

[24] T. Reti, L. Horvath and I. Felde. A comparative study of methods used for the prediction of nonisothermal austenite decomposition. *J. of materials engineering and performance*, **6 (4)**, 433–441, 1997.

[25] D. Rosenthal. Mathematical theory of heat distribution during welding and cutting. *Welding Journal*, **20**, 220–234, 1941.

[26] E. Scheil. Anlaufzeit der austenitumwandlung. *Arch. Eisenhuettenwes.*, **12**, 565–567, 1935.

[27] W. Schulz, V. Kostrykin, H. Zefferer, D. Petring and R. Poprawe. A free boundary problem related to laser beam fusion cutting: Ode approximaton. *Int. J. Heat Mass Transfer*, **40**(12), 2913–2928, 1997.

[28] Z. Shen, S. Zhang, J. Lu and X. Ni. Mathematical modelling of laser induced heating and melting in solids. *Optics and Laser Technology*, **40**(8), 533–537, 2001.

[29] P. S. Sheng and V. S. Joshi. Analysis of heat-affected zone formation for laser cutting of stainless steel. *J. Material Processing Technology*, **53**, 879–892, 1995.

[30] M. Storti. Numerical modelling of ablation phenomena as two-phase Stefan problems. *Int.J.Heat Mass Transfer*, **38**(15), 2843–2854, 1995.

[31] B. An Ton. A Stefan-Signorini problem with set-valued mappings in domains with intersecting fixed and free boundaries. *Bollettino U.M.I.*, **7**, 231–249, 1994.

[32] F. Wever and O. Krisement. Anlaufziet der Austenitumwandlung bei verschiedener Art der Abkühlung. *Archiv für das Eisenhüttenwesen*, **23**, 229–237, 1952.